

Origin of the broad-band noise in acoustic cavitation

Kyuichi Yasui

National Institute of Advanced Industrial Science and Technology (AIST), Nagoya 463-8560, Japan

ARTICLE INFO

Keywords:

Broad-band noise
Acoustic cavitation
Shock wave emission
Chaotically pulsating bubbles
Temporal fluctuation in number of bubbles
Numerical simulations

ABSTRACT

The broad-band noise has been experimentally used to monitor the cavitation activity in a sonochemical reactor, an ultrasonic cleaning bath, a biological tissue, etc. However, the origin of the broad-band noise is still under debate. In the present review, two models for the mechanism of the broad-band noise are discussed. One is acoustic emissions from chaotically (non-periodically) pulsating bubbles. The other is acoustic emissions from bubbles with temporal fluctuation in the number of bubbles. It is suggested that the latter mechanism is sometimes dominant. Further studies are required on the role for bubble cluster dynamics as well as the bubble–bubble interaction in the broad-band noise especially at relatively low ultrasonic frequencies.

1. Introduction

Acoustic cavitation noise is experimentally observed by using a hydrophone or a special sensor which is resistant to cavitation damage [1–36]. The frequency spectra of acoustic cavitation noise typically consist of a peak at the frequency of the driving ultrasound (f_0), those at its harmonics (nf_0 , where n is integer larger than 1), subharmonics (f_0/n , where n is integer larger than 1), and ultra-harmonics (mf_0/n , where n and m are integers larger than 1 but $n > mandn/m$ is not integer) as well as the continuum component called the broad-band noise [1,9,10,13,15,16,18–20,24,25,30,32–36]. The broad-band noise has been used to monitor the cavitation activity in a sonochemical reactor, an ultrasonic cleaning bath, a biological tissue, etc. [2–9,11–13,15–20,22–24,26–31]. The broad-band noise is often considered to be a result of inertial cavitation which is cavitation with significant bubble growth and subsequent violent bubble collapse caused by the inertia of the inflowing liquid [1–3,11–13,15–17,20–24]. However, detailed mechanism for the broad-band noise is still under debate [32,34,37,38]. One model is the shock wave emissions from cavitation bubbles into the surrounding liquid because the frequency spectrum of the delta function (like an acoustic signal due to a shock wave) is broadband [39]. However, as is shown in section 4, temporally periodic emissions of shock waves without variation in shock wave amplitude and emission timings result in the frequency spectra consisting of driving frequency and its harmonics without broad-band noise. Another model is variation in shock wave amplitudes as well as multi-fronted shock waves produced by the collapses of bubble clusters especially at relatively low ultrasonic frequencies [34]. Another one is

acoustic emissions from chaotically (non-periodically) pulsating bubbles [40]. Another one is nonlinear propagation of an acoustic wave in a bubbly liquid with strong bubble–bubble interaction [41]. The other model is acoustic emissions from cavitation bubbles with temporal fluctuation in the number of bubbles [42]. In the present review, origin of the broad-band noise is discussed both theoretically and experimentally.

2. What is acoustic cavitation noise?

In acoustic cavitation, bubbles created by the irradiation of strong ultrasound pulsate strongly [43]. During the rarefaction phase of the driving ultrasound, bubbles expand. During the compression phase of ultrasound, some bubbles collapse very violently, which is called the Rayleigh collapse [43,44]. There are two reasons for the violent collapse of a bubble [43,45]. One is the inertia of the inflowing liquid. The other is the (nearly) spherical geometry of the bubble collapse because the magnitude of the inflowing velocity of the liquid increases as the surface area of a bubble decreases according to the equation of continuity of the liquid. The violent collapse of a bubble stops when the internal gas pressure of a bubble increases significantly as the internal gas density nearly reaches that of the condensed phase. At the final moment of the bubble collapse, temperature and pressure inside a bubble significantly increase to thousands of Kelvin and hundreds of atmospheric pressure or more, respectively [43–48]. As a result, a faint light is emitted and chemical reactions occur inside a bubble, which are called sonoluminescence and sonochemical reactions, respectively [48,49].

Like the sound radiation from a vibrating diaphragm of a loud-

E-mail address: k.yasui@aist.go.jp.

<https://doi.org/10.1016/j.ultsonch.2022.106276>

Received 31 October 2022; Received in revised form 30 November 2022; Accepted 21 December 2022

Available online 24 December 2022

1350-4177/© 2022 The Author(s). Published by Elsevier B.V. This is an open access article under the CC BY-NC-ND license (<http://creativecommons.org/licenses/by-nc-nd/4.0/>).

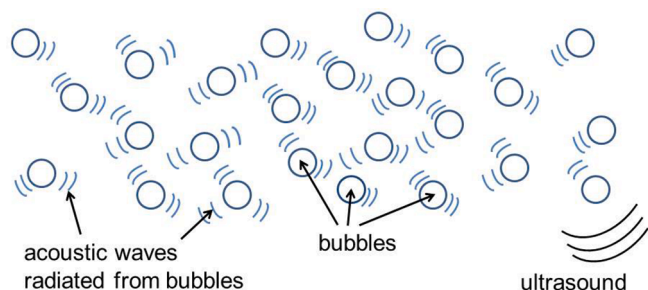


Fig. 1. Acoustic waves radiated from cavitation bubbles (acoustic cavitation noise) [50]. Reprinted with permission from Handbook of Ultrasonics and Sonochemistry, Springer, edited by M. Ashokkumar et al., vol. 1, K. Yasui, Unsolved problems in acoustic cavitation, pp. 259–292, Copyright (2016), Springer.

speaker, pulsating bubbles radiate acoustic waves into the surrounding liquid, which is called the acoustic cavitation noise (Fig. 1) [50]. Typical frequency spectra of acoustic cavitation noise are shown in Fig. 2 for various acoustic intensities [1]. At a very low acoustic intensity, only a peak at the frequency of the driving ultrasound is observed (0 and 1 of

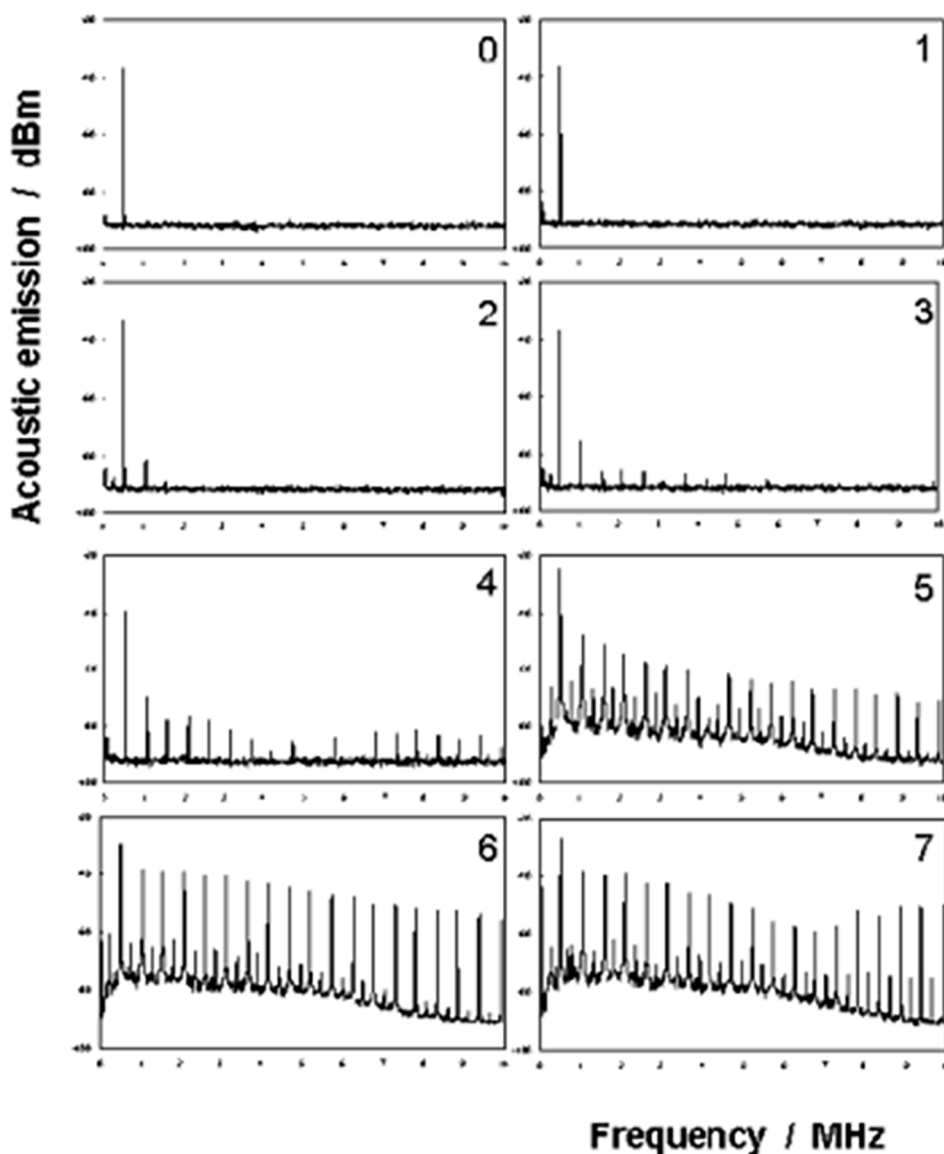


Fig. 2. Experimentally observed spectra of acoustic cavitation noise at different applied acoustic intensities [1]. 0, 0 W cm⁻², 1, <0.05 W cm⁻², 2, 0.05 W cm⁻², 3, 0.08 W cm⁻², 4, 0.54 W cm⁻², 5, 0.7 W cm⁻², 6, 2.2 W cm⁻², 7, 6.8 W cm⁻². Reprinted with permission from J. Am. Chem. Soc., vol. 129, M. Ashokkumar, M. Hodnett, B. Zeqiri, F. Grieser, G.J. Price, Acoustic emission spectra from 515 kHz cavitation in aqueous solutions containing surface-active solutes, pp. 2250–2258, Copyright (2007), American Chemical Society.

Fig. 2). At the threshold for sonoluminescence and sonochemical reactions (4 of Fig. 2), peaks at the harmonics of the driving frequency are observed. At acoustic intensities considerably above the threshold (5–7 in Fig. 2), peaks at half-order subharmonic ($f_0/2$) and ultra-harmonics ($(2n-1)f_0/2$) as well as the broad-band noise are also observed.

Surprisingly, for low concentration surfactant solutions (0.5–2 mM SDS solutions), only harmonics were observed and broad-band noise as well as the subharmonic and ultra-harmonics disappeared even considerably above the threshold for sonoluminescence and sonochemical reactions (Fig. 3) [1]. This experimental observation provides useful information on the origin of the broad-band noise [42]. This is discussed in section 4.

In acoustic cavitation, there are many cavitation bubbles and there is strong bubble–bubble interaction which is the effect of acoustic waves radiated from surrounding bubbles on the pulsation of a bubble [42,43,50–55]. Furthermore, shielding of the driving ultrasonic wave occurs by the surrounding bubbles. Such the complexities are eliminated for a single-bubble system in which a single bubble is trapped near the pressure antinode of a standing ultrasonic wave by the radiation force and pulsates stably in a moderately degassed water [44,56,57]. Sonoluminescence from a single-bubble system is called single-bubble sonoluminescence (SBSL) [44,58,59]. Difference and similarity

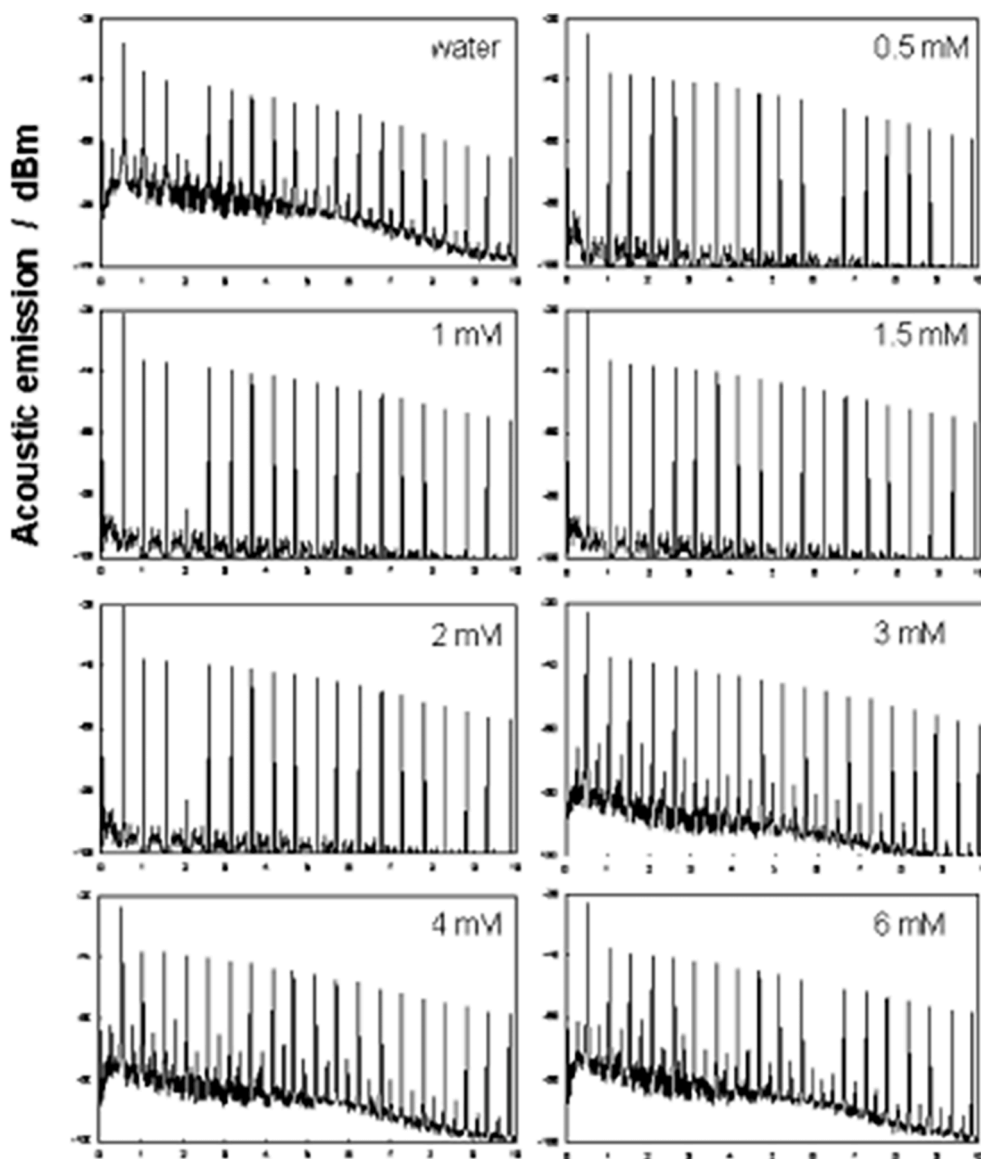


Fig. 3. Experimentally observed spectra of acoustic cavitation noise from aqueous solutions containing different concentration of SDS (surfactant) at 515 kHz with the acoustic intensity of 2.2 W cm^{-2} [1]. Reprinted with permission from J. Am. Chem. Soc., vol. 129, M. Ashokkumar, M. Hodnett, B. Zeqiri, F. Grieser, G.J. Price, Acoustic emission spectra from 515 kHz cavitation in aqueous solutions containing surface-active solutes, pp. 2250–2258, Copyright (2007), American Chemical Society.

between SBSL and multibubble sonoluminescence (MBSL), which is sonoluminescence from many bubbles in acoustic cavitation, with respect to the light emission mechanism are still under debate [48].

Matula et al. [57] experimentally observed acoustic emissions from a single-bubble system (Fig. 4). The acoustic signals were observed at the end of each bubble collapse, especially at the end of the violent collapse (the first collapse). At the end of the violent collapse, a spherical shock wave is radiated from a bubble into the surrounding liquid (Fig. 5) [60,61]. Thus, the acoustic signal at the end of the violent collapse is due to the shock wave. In a multibubble system, Negishi [62] experimentally observed strong acoustic signals at each violent collapse of bubbles. These acoustic signals are also due to the shock waves radiated from cavitation bubbles.

The reason for the shock wave emission from a bubble at the end of the violent collapse is as follows. In Fig. 6, the numerically calculated spatial variation of pressure in the liquid is shown at different instants in time during the bubble collapse (left figure) and the rebound (right

figure) [63]. The dotted line shows the position of the bubble wall at different instants in time. The time indicated in the figure is $(t-\tau)10^4/\tau$, where τ is the time required for the bubble to collapse from the initial radius to the final minimum radius and t is the time elapsed from the start of the motion [63]. In other words, the time at the end of the violent collapse is 0. During the bubble collapse (rebound), the time is negative (positive). During the bubble collapse (left figure), there is no shock wave emission into the liquid. During the rebound (right figure), a shock wave is formed in the liquid because of the following reason. Pressure disturbances propagate from the bubble wall into the surrounding liquid with the sound speed plus the local fluid (liquid) velocity. The local fluid (liquid) velocity is directed outward during the rebound, and its magnitude decreases as the distance from the bubble wall increases. Accordingly, the pressure disturbances emitted from the bubble wall overtake the previously emitted ones. As a result, a sharp shock wave is formed in the liquid. It should be noted that the Mach number of the liquid velocity is less than 0.2 during the rebound, and the shock

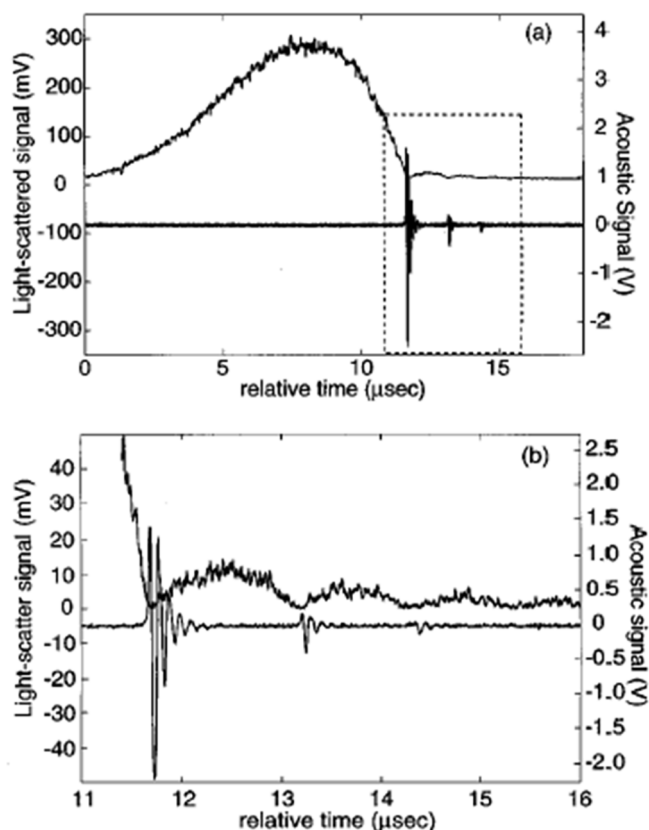


Fig. 4. Experimental results for a stably pulsating bubble under the condition of single-bubble sonoluminescence (33.8 kHz) [57]. (a) The radius-time curve measured by laser light scattering with the corresponding acoustic signals. (b) A detailed view of the boxed area in (a). The acoustic data is shifted in time equal to the time necessary for sound to travel from the bubble to the transducer, about 16.77 μ s. Reprinted with permission from J. Acoust. Soc. Am., vol. 103, T. J. Matula, I.M. Hallaj, R.O. Cleveland, L.A. Crum, W.C. Moss, R.A. Roy, The acoustic emissions from single-bubble sonoluminescence, pp. 1377–1382, Copyright (1998), Acoustical Society of America.

formation from the rebounding bubble is not originated in a large Mach number [63]. In general, shock waves can be formed under relatively low Mach numbers although Mach number should be larger than 1 for a shock wave propagation in a homogeneous medium under steady-state conditions according to the Rankine-Hugoniot relations [64–66].

3. Chaotic (non-periodic) pulsation of bubbles

It has long been believed that the broad-band noise is originated in

chaotic (non-periodic) pulsation of bubbles. Chaotically (non-periodically) pulsating bubbles radiate acoustic waves into the liquid with temporally non-periodical variation in acoustic pressure (Fig. 7) [40]. Chaotic pulsation of a bubble originates in the nonlinear nature of bubble pulsation. Indeed, bubble pulsation (radius-time curve) is mathematically described by the nonlinear Rayleigh-Plesset equation or Keller equation, etc. [43]. The nonlinearity is originated in asymmetric nature of bubble expansion and contraction (collapse). As the compression of liquid is harder than that of gas, bubble expansion is more difficult than bubble contraction (collapse). In other words, bubble expansion is much milder than bubble collapse.

Lauterborn et al. [25,67–69] have shown both experimentally and theoretically that spectra of acoustic cavitation noise exhibited the period-doubling bifurcation to chaos as the pressure amplitude of the driving ultrasound increases due to the nonlinear nature of the bubble pulsation. Period-doubling bifurcation is known in many nonlinear systems and is characterized by the appearance of half-frequency component (at lower subharmonic frequency) and its harmonics (ultra-harmonics) [70]. In general, an infinite sequence of period-doubling bifurcations is a route to chaos as a control parameter increases [70]. Chaos occurs in strongly nonlinear systems, which exhibits non-periodic motion and small difference in the initial condition results in huge difference after some time [70]. Lauterborn and Cramer [25] found experimentally that spectra of acoustic cavitation noise exhibited the period-doubling bifurcation to chaos as the voltage applied to the transducer, which radiates the driving ultrasound (22.6 kHz) into the liquid, increased. Lauterborn and Suchla [67] showed by numerical simulations that bubble pulsation under ultrasound of 23.6 kHz exhibited the period-doubling bifurcation to chaos as the pressure amplitude of the driving ultrasound increased to about 6 bar (Fig. 8). In the numerical simulations, the pressure amplitude of the driving ultrasound was increased from 0 to 14.8 bar in 40 ms [67]. After about 20 ms (7.4 bar), a second sequence of the period-doubling bifurcation to chaos was observed (Fig. 8).

However, the problem of the numerical simulations shown in Fig. 8 is the assumed ambient bubble-radius (R_0), which is the bubble radius in the absence of ultrasound, of 100 μ m. According to the numerical simulations of bubble shape oscillations [71], a bubble of $R_0 = 100 \mu$ m becomes shape unstable and disintegrates into daughter bubbles after a few acoustic cycles above about 1 bar in pressure amplitude of the driving ultrasound (Fig. 9). In the numerical simulations shown in Fig. 8, the effect of bubble shape instability was completely neglected. In the next section, it is shown that the effect of bubble shape instability plays a crucial role in broad-band component of acoustic cavitation noise.

4. Temporal fluctuation in number of bubbles

In the present section, the experimental results in Fig. 3 are discussed based on the numerical simulations of acoustic cavitation noise [42]. It has been experimentally reported that in low concentration surfactant

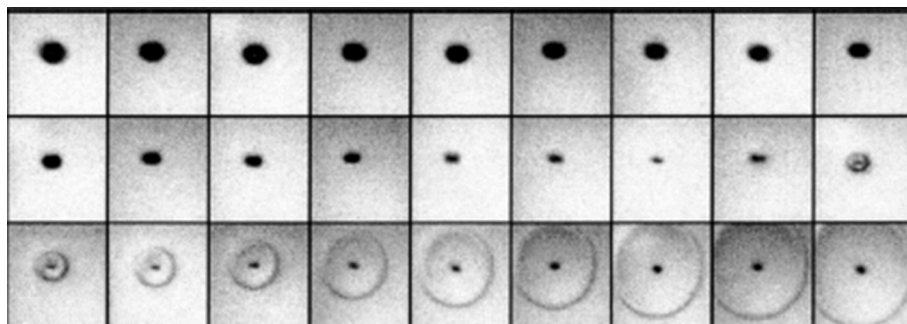


Fig. 5. Collapse and rebound of a laser-produced spherical bubble in water, experimentally observed at 20.8 million frames per second (48-ns interframe time) with shock wave emission [60]. The size of the picture is 1.5 \times 1.8 mm. Reprinted with permission from Advances in Chemical Physics, John Wiley & Sons, edited by I. Prigogine, S.A. Rice, vol. 110, W. Lauterborn, T. Kurz, R. Mettin, C.D. Ohl, Experimental and theoretical bubble dynamics, pp. 295–380, Copyright (1999), John Wiley & Sons.

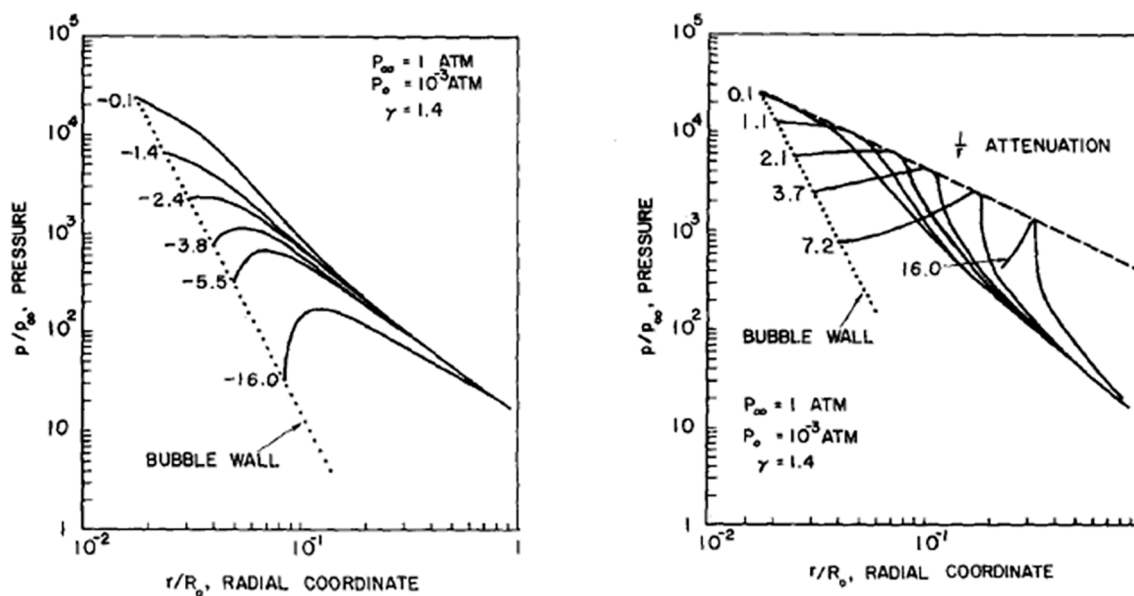


Fig. 6. Results of numerical simulations for collapse (left) and rebound (right) of a spherical bubble in water on spatial distributions of pressure in the liquid for different instants in time [63]. A shock wave is radiated from a bubble into the surrounding liquid during the rebound (right). Reprinted with permission from Physics of Fluids, vol. 7, R. Hickling, M.S. Plesset, Collapse and rebound of a spherical bubble in water, pp. 7–14, Copyright (1964), AIP Publishing.

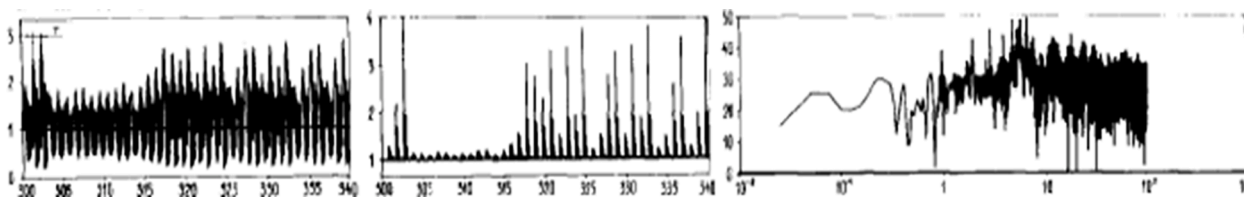


Fig. 7. Results of numerical simulations for chaotic pulsation of a bubble on radius-time curve (left), radiated acoustic signal (center), and frequency spectrum of the acoustic signal (right) at 31 kHz and 0.9929 atm in ultrasonic frequency and pressure amplitude, respectively, with the ambient bubble radius of 20 μm [40]. Reprinted with permission from Ultrasonics, vol. 27, V.I. Ilyichev, V.L. Koretz, and N.P. Melnikov, Spectral characteristics of acoustic cavitation, pp. 357–361, Copyright (1989), Elsevier.

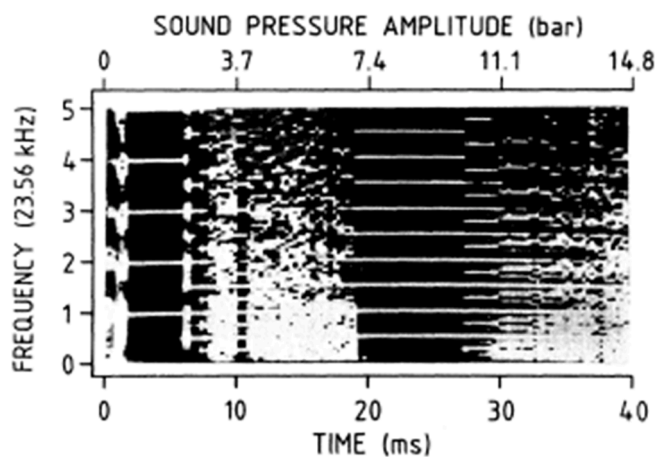


Fig. 8. Results of numerical simulations for bubble pulsation at 23.56 kHz with the ambient bubble radius of 100 μm [67]. The acoustic pressure amplitude is raised from 0 to 14.8 bar in 40 ms. The frequency spectra of bubble pulsation are shown as a function of acoustic pressure amplitude. Reprinted with permission from Phys. Rev. Lett., vol. 53, W. Lauterborn, E. Suchla, Bifurcation superstructure in a model of acoustic turbulence, pp. 2304–2307, Copyright (1984), American Physical Society.

solutions (1.5 mM SDS) the typical ambient bubble-radius is considerably smaller than that in pure water (Fig. 10) [72]. The reason is the considerable retardation in coalescence of bubbles in the presence of low concentration surfactant [73]. Typical range of ambient bubble radius in low concentration surfactant solution (1.5 mM SDS) is from 0.9 μm to 1.7 μm , while that in pure water is from 2.8 μm to 3.7 μm (Fig. 10) [72]. The range of ambient bubble radius was experimentally determined by the decrease of sonoluminescence intensity by increasing the pulse-off time of pulsed ultrasound. Increasing the pulse-off time, larger bubbles completely dissolve into the liquid during the pulse-off time. Accordingly, the sonoluminescence intensity during the pulse-on time decreases because the total number of bubbles decreases. By changing the pulse-off time, relative number of bubbles of the specific size is obtained by calculating the time for complete dissolution of a bubble of a specific size into the liquid [72].

Numerical simulations of acoustic cavitation noise were performed under the conditions of the experiment in Fig. 3 (515 kHz and 2.6 bar in ultrasonic frequency and pressure amplitude of the driving ultrasound, respectively) [42]. For 1.5 mM SDS solution, the ambient bubble radius is assumed as $R_0 = 1.5 \mu\text{m}$ according to the experimental results in Fig. 10. Under the condition, shape oscillation of a bubble is gradually damped due to the small ambient radius of a bubble (Fig. 11(a)) [42]. In other words, a bubble is shape stable and does not disintegrate into daughter bubbles. Accordingly, there is no temporal fluctuation in number of bubbles. Under the condition, radius-time curve is accurately periodic with the acoustic period (Fig. 11(b)) [42]. The pressure of

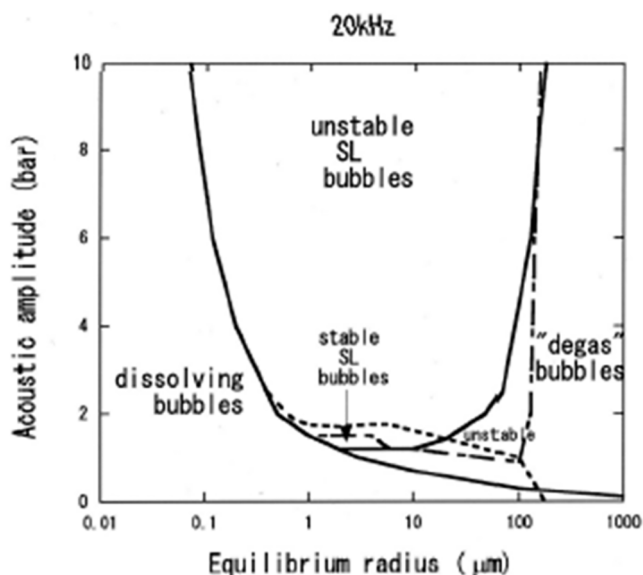


Fig. 9. Results of numerical simulations for bubble pulsation at 20 kHz with various acoustic pressure-amplitudes and various ambient bubble radii [71]. Above the dash-dotted line, a bubble disintegrates into daughter bubbles in a few acoustic cycles or a few tens of acoustic cycles. Above the dotted line, a bubble is repelled from the pressure antinode of a standing wave of ultrasound. Reprinted with permission from J. Acoust. Soc. Am., vol. 112, K. Yasui, Influence of ultrasonic frequency on multibubble sonoluminescence, pp. 1405–1413, Copyright (2002), Acoustical Society of America.

acoustic wave radiated from bubbles is dominated by pressure pulses due to shock waves emitted from bubbles (Fig. 11(c)) [42]. The pressure pulses are emitted periodically with time because the radius-time curve is accurately periodic. The hydrophone signal (U) is numerically simulated as follows [42,74].

$$\ddot{U} + 2\gamma\pi f_c \dot{U} + 4\pi^2 f_c^2 U = P(t) + p_s(t) \quad (1)$$

where γ is the coefficient for damping, f_c is the characteristic frequency of the hydrophone, $P(t)$ is the instantaneous pressure of acoustic waves radiated from bubbles, and $p_s(t)$ is the instantaneous pressure of the driving ultrasound. In the numerical simulations, $f_c = 5$ MHz and $\gamma = 1$

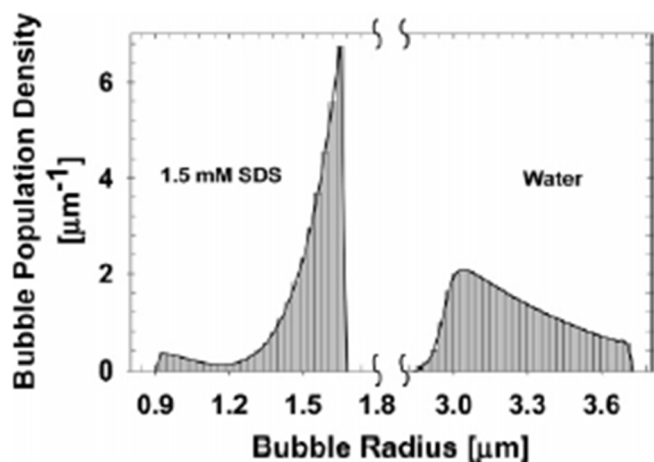


Fig. 10. Experimental results on size distribution of sonoluminescing bubbles measured by changing the pulse-off time of pulsed ultrasound for water and 1.5 mM SDS (surfactant) solution [72]. Reprinted with permission from J. Am. Chem. Soc., vol. 127, J. Lee, M. Ashokkumar, S. Kentish, F. Grieser, Determination of the size distribution of sonoluminescence bubbles in a pulsed acoustic field, pp. 16810–16811, Copyright (2005), American Chemical Society.

are assumed [42]. $P(t)$ is given as follows.

$$P = S\rho(R^2\ddot{R} + 2R\dot{R}^2) \quad (2)$$

$$S = \sum_{i=1}^N \frac{1}{r_i} \quad (3)$$

where S is called the coupling strength because it is related to the strength of the bubble–bubble interaction, ρ is the liquid density, R is the instantaneous bubble radius, dot denotes the time derivative (d/dt), r_i is the distance from the bubble numbered i to the hydrophone, and N is the total number of bubbles. In the derivation of Eq. (2), it is assumed that bubbles are spatially uniformly distributed and the ambient bubble radii of all the bubbles are the same. The coupling strength (S) is approximately given as follows [43,51–53].

$$S = \int_{l_{min}}^{l_{max}} \frac{4\pi r^2 n}{r} dr = 2\pi n(l_{max}^2 - l_{min}^2) \approx 2\pi n l_{max}^2 \quad (4)$$

where l_{max} is the radius of a bubble cloud, l_{min} is the distance from a nearest bubble, $l_{max} \gg l_{min}$ is assumed in the last equation, and n is the number density of bubbles.

The numerically simulated hydrophone signal in Fig. 11(d) is also a periodic function of time, which mainly consists of sharp signals due to shock waves superimposed on nearly sinusoidal wave due to the driving ultrasound [42]. Accordingly, the frequency spectrum of the hydrophone signal only consists of the peak at the driving frequency and those at its harmonics without broad-band noise because any periodic function is expressed by a Fourier series consisting of fundamental frequency and its harmonics [75]. It should be noted that periodic shock-wave emissions without variation in shock wave amplitude and emission timings result in harmonics without broad-band noise. In other words, shock waves do not necessarily result in the broad-band noise although many researchers have regarded shock waves emitted from cavitation bubbles as the origin of the broad-band noise. It should also be noted that the effect of surface tension and surface dilatational viscosity of the surfactant (SDS) is negligible on the spectra of acoustic cavitation noise [42].

Next, acoustic cavitation noise from pure water is numerically simulated under the condition of the experiment of Fig. 3 (Fig. 12) [42]. For pure water, the ambient bubble radius is assumed as $R_0 = 3\mu\text{m}$ according to the experimental result of Fig. 10. In this case, a bubble is shape unstable and disintegrates into daughter bubbles after about four acoustic cycles as the shape oscillation amplitude exceeds the instantaneous bubble radius after about four acoustic cycles [42]. Then, number of bubbles temporally fluctuates. This is taken into account in the numerical simulations by the temporal variation of the coupling strength (S) as follows.

$$S(t+T) = S(t) + (\Delta S)r_n \quad (5)$$

where $S(t+T)$ and $S(t)$ are the coupling strength at time $t+T$ and t , respectively, T is the acoustic period, ΔS is the maximum amplitude of the temporal variation of S per acoustic cycle, and r_n is a random number generated by a computer from -1 to 1 . In the numerical simulations, $\Delta S = S_0/L$ is assumed, where S_0 is the initial coupling strength and L is the lifetime of a bubble expressed in acoustic cycle ($L = 4$ in the case of Fig. 12). The temporal variation of S generated by a computer is shown in Fig. 12(a) [42].

The coupling strength (S) influences the radius-time curve of a bubble through the bubble–bubble interaction as follows [43].

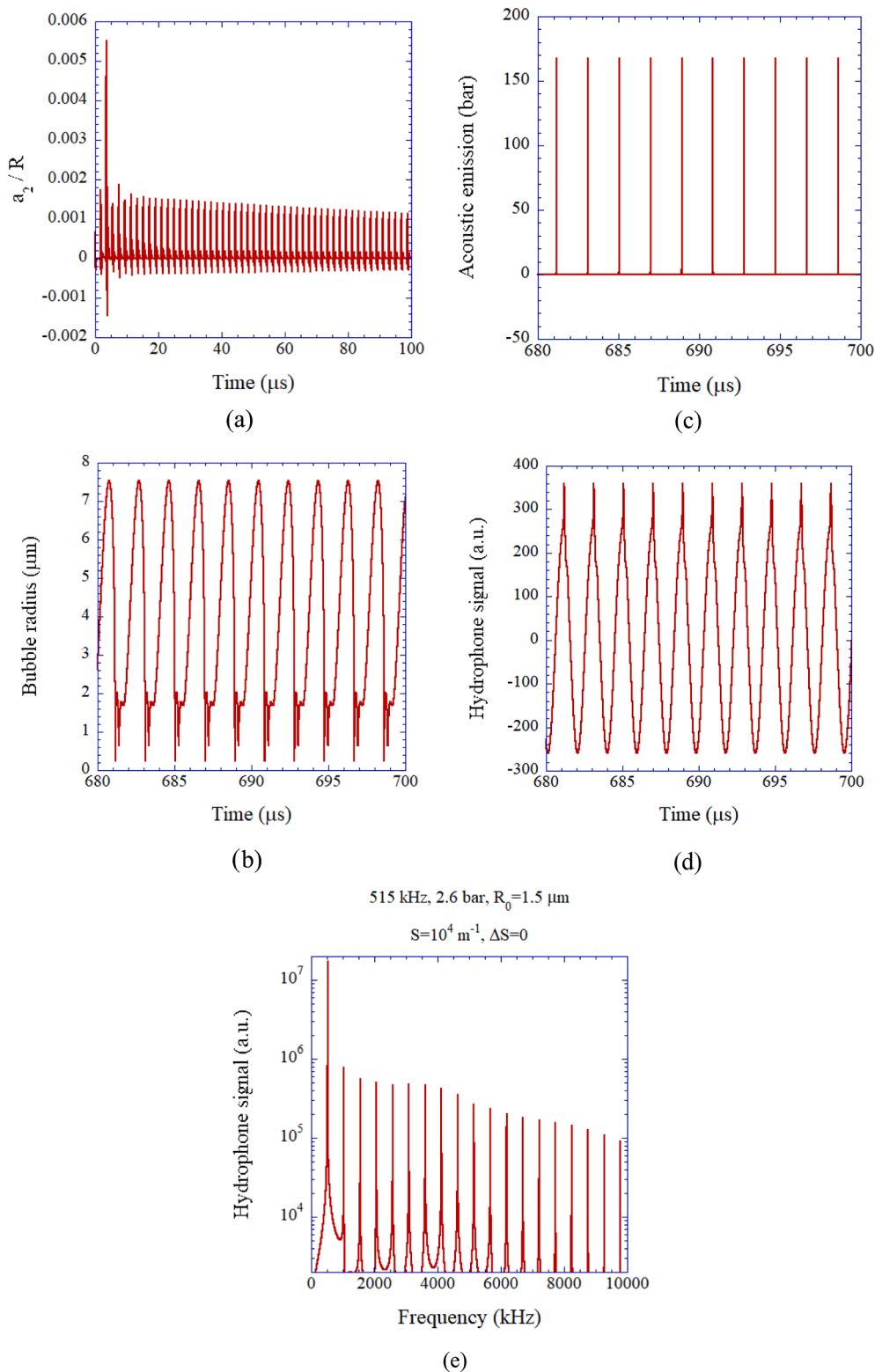


Fig. 11. Results of numerical simulations of bubble pulsation and acoustic emissions with the ambient bubble radius of 1.5 μm which is typical in low-concentration SDS solution under 515 kHz and 2.6 bar in ultrasonic frequency and acoustic pressure amplitude, respectively [42]. There is no temporal fluctuation in number of bubbles because bubbles are shape stable. (a) The amplitude of non-spherical component ($n = 2$) of the bubble shape relative to the instantaneous bubble radius (R) for the initial 100 μs. (b) The bubble radius (R) as a function of time. (c) The pressure of acoustic waves radiated from bubbles as a function of time. (d) The hydrophone signal in arbitrary unit as a function of time. (e) The frequency spectrum of the hydrophone signal with the logarithmic vertical axis. Reprinted with permission from Ultrason. Sonochem., vol. 17, K. Yasui, T. Tuziuti, J. Lee, T. Kozuka, A. Towata, Y. Iida, Numerical simulations of acoustic cavitation noise with the temporal fluctuation in the number of bubbles, pp. 460–472, Copyright (2010), Elsevier.

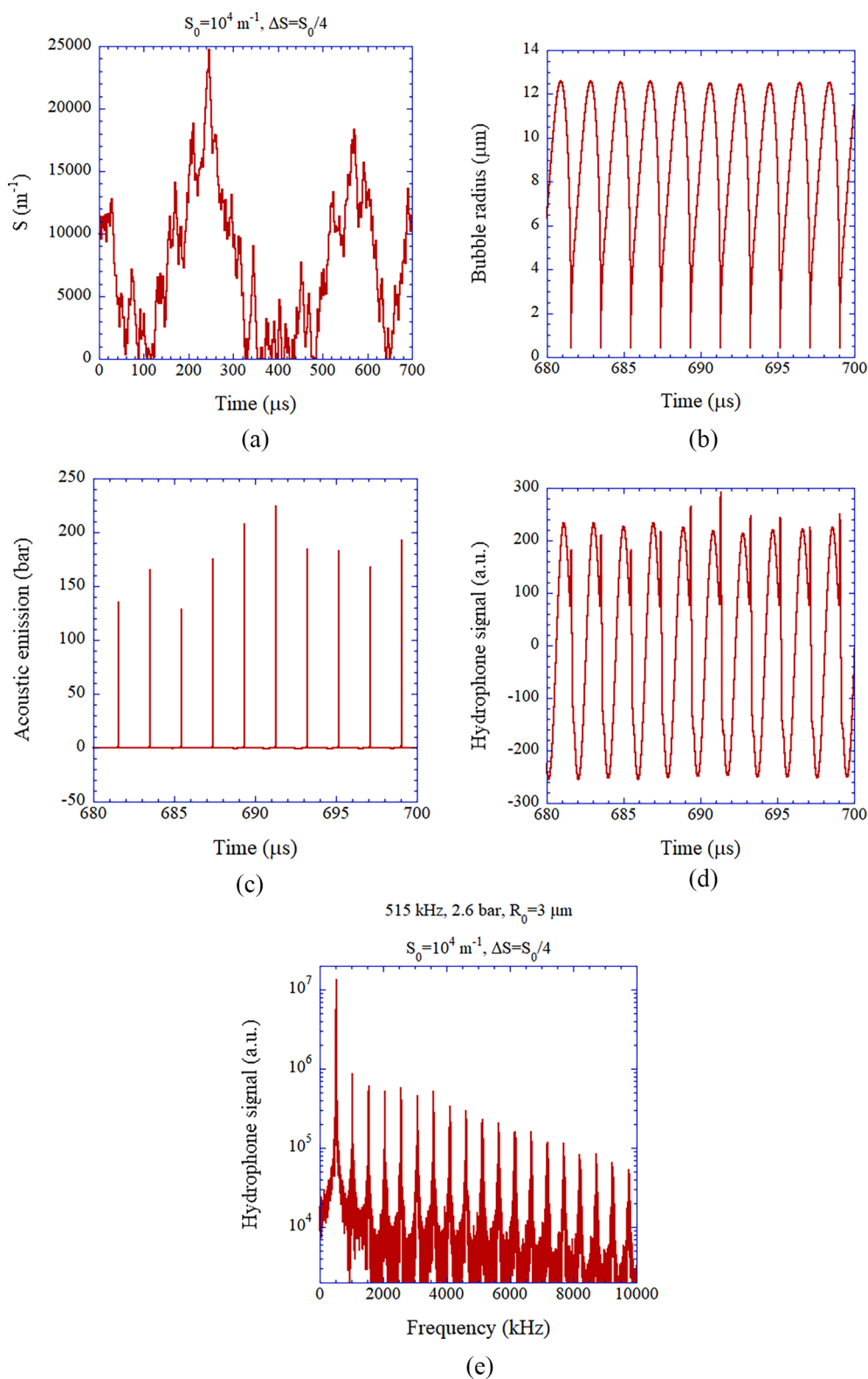


Fig. 12. Results of numerical simulations of bubble pulsation and acoustic emissions with the ambient bubble radius of $3 \mu\text{m}$ which is typical in pure water under 515 kHz and 2.6 bar in ultrasonic frequency and acoustic pressure amplitude, respectively [42]. There is temporal fluctuation in number of bubbles because a bubble disintegrates into daughter bubbles in 4 acoustic cycles. (a) The randomly varying “coupling strength” as a function of time generated by a computer. The time axis is from 0 to 700 μs . (b) The bubble radius (R) as a function of time. (c) The pressure of acoustic waves radiated from bubbles as a function of time. (d) The hydrophone signal in arbitrary unit as a function of time. (e) The frequency spectrum of the hydrophone signal with the logarithmic vertical axis. Reprinted with permission from Ultrason. Sonochem., vol. 17, K. Yasui, T. Tuziuti, J. Lee, T. Kozuka, A. Towata, Y. Iida, Numerical simulations of acoustic cavitation noise with the temporal fluctuation in the number of bubbles, pp. 460–472, Copyright (2010), Elsevier.

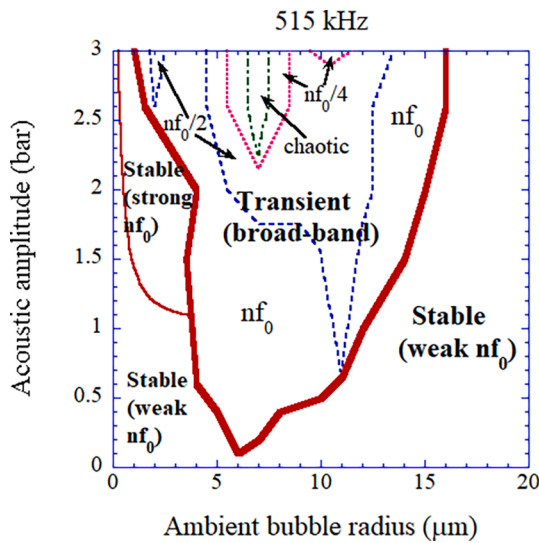


Fig. 13. Results of numerical simulations of bubble pulsation at 515 kHz with various acoustic pressure amplitudes and various ambient bubble radii [42]. The regions for “transient” cavitation bubbles and “stable” cavitation bubbles are shown in the parameter space of ambient bubble radius and the acoustic pressure amplitude. “Stable” (“transient”) cavitation bubbles are defined as those which are shape stable (unstable). The thickest line is the border between the region for “stable” cavitation bubbles and that for “transient” ones. The type of bubble pulsation is indicated as chaotic (non-periodic), periodic with the acoustic period (denoted as nf_0 because of the noise spectra consisting of the driving frequency and its harmonics), doubled acoustic period (denoted as $nf_0/2$ because of the noise spectra consisting of the driving frequency, its harmonics, half-order subharmonic, and ultraharmonics), and quadrupled acoustic period (denoted as $nf_0/4$ because of the noise spectra consisting of the driving frequency, its harmonics, the half-order subharmonic, and ultraharmonics ($nf_0/4$)). Reprinted with permission from Ultrason. Sonochem., vol. 17, K. Yasui, T. Tuziuti, J. Lee, T. Kozuka, A. Towata, Y. Iida, Numerical simulations of acoustic cavitation noise with the temporal fluctuation in the number of bubbles, pp. 460–472, Copyright (2010), Elsevier.

$$\left(1 - \frac{\dot{R}}{c_\infty}\right) R\ddot{R} + \frac{3}{2}\dot{R}^2 \left(1 - \frac{\dot{R}}{3c_\infty}\right) = \frac{1}{\rho_{L,\infty}} \left(1 + \frac{\dot{R}}{c_\infty}\right) (p_B + A \sin \omega t - p_\infty) + \frac{R}{c_\infty \rho_{L,\infty}} \frac{dp_B}{dt} - S(2R\dot{R}^2 + R^2\ddot{R}) \quad (6)$$

where c_∞ is the sound velocity in liquid at ambient condition, $\rho_{L,\infty}$ is the liquid density at ambient condition, p_B is the liquid pressure at the bubble wall, A and ω are the pressure amplitude and the angular frequency of the driving ultrasound, respectively, and p_∞ is the ambient pressure. The last term of Eq. (6) is the pressure of acoustic waves radiated by surrounding bubbles divided by $\rho_{L,\infty}$ neglecting the term in the order of $(R/r)(\dot{R}/c_\infty)$. The last term is the effect of the bubble–bubble interaction. When the term is omitted, Keller equation is recovered [43].

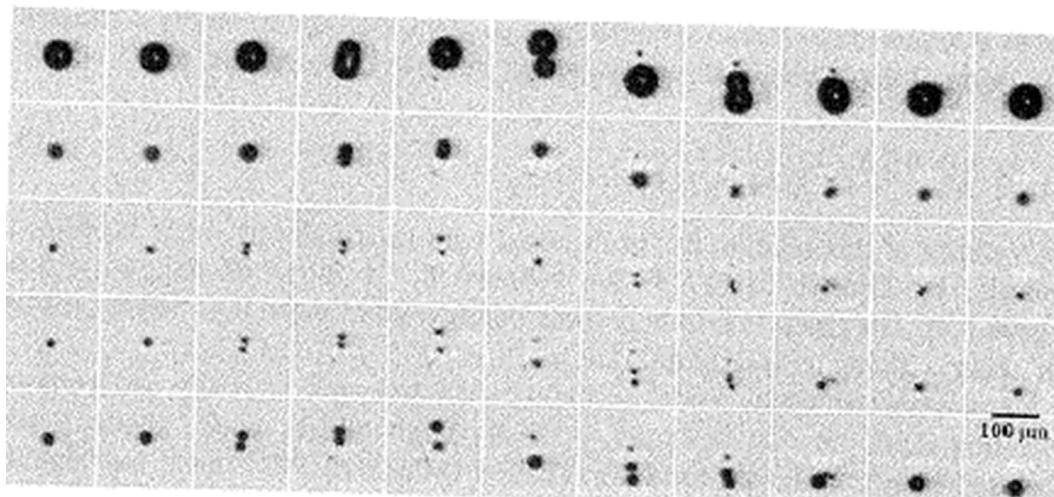
In spite of the bubble–bubble interaction, the radius-time curve is nearly periodic with the acoustic period (Fig. 12(b)) [42]. However, the pressure of acoustic waves radiated from bubbles is no longer periodic because the height of each peak is proportional to the coupling strength

(S) (Eq. (2)) and S temporally fluctuates as shown in Fig. 12(a) (Fig. 12(c)). In other words, the acoustic signal from bubbles is no longer periodic as a function of time because number of bubbles temporally fluctuates and accordingly the number of shock waves radiated from bubbles temporally fluctuates. Then, the hydrophone signal is no longer periodic with time because the height of the peaks due to shock waves fluctuates with acoustic cycles (Fig. 12(d)). As a result, the broad-band noise appears in the frequency spectrum of the hydrophone signal because non-periodic component in a time series results in the broad-band component in the frequency spectrum (Fig. 12(e)) [42]. In conclusion, temporal fluctuation in number of bubbles results in the broad-band noise [42]. According to Seya et al. [27], temporal fluctuation in the bubble size distribution also results in the broad-band noise. It is partly due to the variation in timings of shock wave emissions. It should also be noted that under a relatively high coupling-strength the broad-band noise is intensified by the bubble–bubble interaction [42]. In other words, the broad-band noise is intensified by the bubble–bubble interaction when the number density of bubbles is relatively high. It is related to the broad-band noise resulted from the nonlinear propagation of an acoustic wave in a bubbly liquid with strong bubble–bubble interaction reported by An [41].

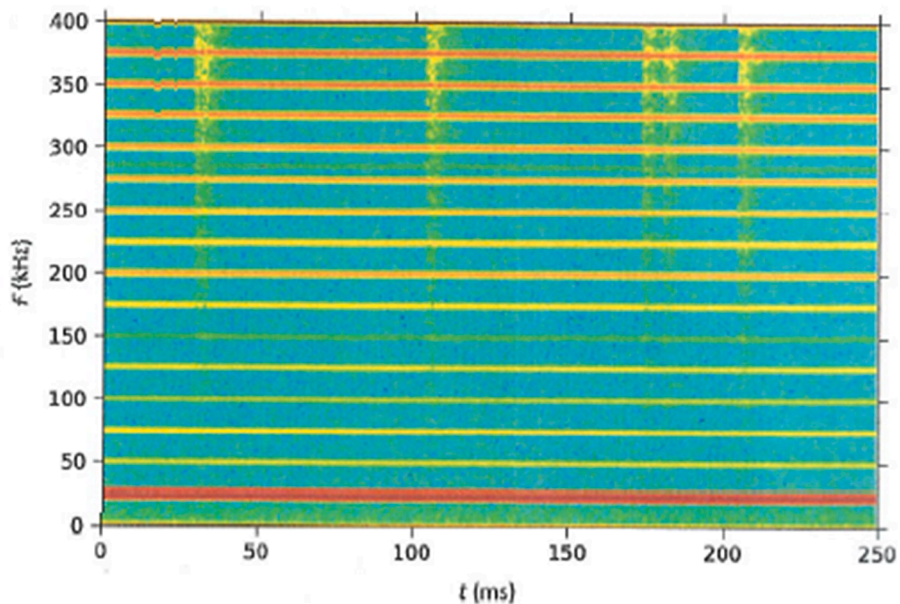
Numerical simulations are performed for various ambient bubble radii and acoustic amplitudes under the experimental condition of Fig. 3 (515 kHz) (Fig. 13). Above the thick solid line in Fig. 13, a bubble disintegrates into daughter bubbles in a few or a few hundred acoustic cycles due to the shape instability. In other words, there is temporal fluctuation in the number of bubbles above the thick solid line, which results in the broad-band noise. On the other hand, the area in the phase space of ambient bubble radius and acoustic amplitude for chaotic (non-periodic) pulsation is very narrow in Fig. 13 [42]. The area for periodic pulsation with quadrupled acoustic period ($nf_0/4$) in the phase space is a little bit larger than that for chaotic pulsation as shown in Fig. 13. In the experimental data of the acoustic cavitation noise from pure water in Fig. 3 at the acoustic amplitude of about 2.6 bar, however, there are no peaks at $(2n-1)/4$. Thus, it is expected that the contribution of chaotic pulsation on the broad-band noise is also negligible at the acoustic amplitude of about 2.6 bar. Furthermore, typical range of ambient bubble radius in the experiment is from 2.8 μm to 3.7 μm (Fig. 10) [72]. In other words, the main mechanism for the broad-band noise under the experimental condition of Fig. 3 is the temporal fluctuation in the number of bubbles. It is expected that broad-band noise is often originated in the temporal fluctuation in the number of bubbles.

Experimentally, Lauterborn and Mettin [76] reported that broad-band noise was observed when a bubble disintegrated into daughter bubbles in a single-bubble system according to the experiment by J. Schneider and J. Eisener (Fig. 14). It is the experimental evidence that temporal fluctuation in the number of bubbles results in the broad-band noise although not only the variation in shock wave amplitudes but also that of emission timings causes the broad-band noise.

Song, Moldovan, and Prentice [32] experimentally showed that the broad-band noise is originated in the variation in shock wave amplitudes and emission timings as shown in Fig. 15. It is confirmed that main acoustic signals from bubbles are shock waves emitted from bubbles. Furthermore, the experimental results suggest that temporal fluctuation in number of bubbles results in the broad-band noise. However, Yusuf, Symes, and Prentice [34] experimentally suggested that variation in shock wave amplitudes as well as multi-fronted shock waves generated from the collapses of bubble clusters result in the broad-band noise at



(a)



(b)

Fig. 14. Experimental results on repeatedly splitting single bubble trapped near the pressure antinode of a standing ultrasonic wave at 25 kHz by J. Schneider and J. Eisener [76]. (a) Optical images of the bubbles. (b) Frequency spectrum of acoustic noise as a function of time. The broad-band noise repeatedly appeared when a bubble is split into daughter bubbles. Reprinted with permission from Power Ultrasonics, edited by J.A. Gallego-Juarez, K.F. Graff, Elsevier, W. Lauterborn, R. Mettin, Acoustic cavitation: bubble dynamics in high-power ultrasonic fields, pp. 37–78, Copyright (2015), Elsevier.

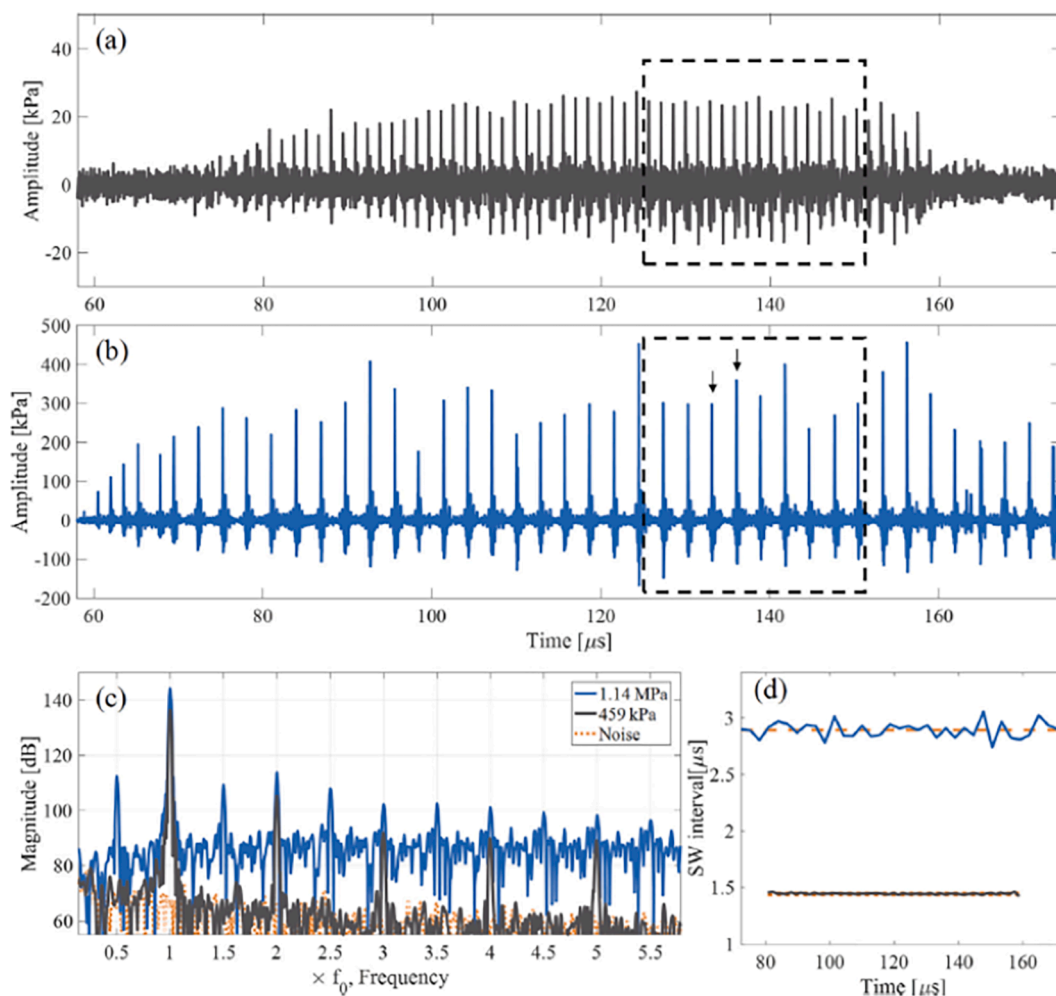


Fig. 15. Experimental results of acoustic cavitation noise driven by a 200-cycle burst of 692 kHz focused ultrasound [32]. (a, b) The needle hydrophone data at peak-negative pressure (PNP) amplitude of 459 kPa (a) and 1.14 MPa (b). (c) The spectra of the signals. (d) Variation in shock wave emission interval times measured from (a) and (b). Reprinted with permission from *Ultrasound Med. Biol.*, vol. 45, J.H. Song, A. Moldovan, P. Prentice, Non-linear acoustic emissions from therapeutically driven contrast agent microbubbles, pp. 2188–2204, Copyright (2019), Elsevier.

relatively low ultrasonic frequencies. Further studies are required on the role for bubble cluster dynamics in the broad-band noise especially at relatively low ultrasonic frequencies [30,77,78].

5. Conclusion

There are mainly-two mechanisms in the origin of the broad-band noise in acoustic cavitation. One is chaotic (non-periodic) pulsation of a bubble. The other is the temporal fluctuation in number of bubbles. Shock wave emissions from bubble do not necessarily result in the broad-band noise because accurately periodic emissions of shock waves without variation in shock wave amplitudes and emission timings result only in harmonics without the broadband noise as any periodic function is expressed by a Fourier series consisting of fundamental frequency and its harmonics. It is suggested that the temporal fluctuation in the number of bubbles is sometimes the origin of the broad-band noise. Further studies are required on the role for bubble cluster dynamics as well as the bubble–bubble interaction in the broad-band noise especially at relatively low ultrasonic frequencies.

CRediT authorship contribution statement

Kyuichi Yasui: Conceptualization, Writing – original draft, Writing – review & editing.

Declaration of Competing Interest

The authors declare that they have no known competing financial interests or personal relationships that could have appeared to influence the work reported in this paper.

Data availability

No data was used for the research described in the article.

Acknowledgments

The author would like to thank his collaborators in his research.

References

- [1] M. Ashokkumar, M. Hodnett, B. Zeqiri, F. Grieser, G.J. Price, Acoustic emission spectra from 515 kHz cavitation in aqueous solutions containing surface-active solutes, *J. Am. Chem. Soc.* 129 (2007) 2250–2258, <https://doi.org/10.1021/ja067960r>.
- [2] B. Zeqiri, N.D. Lee, M. Hodnett, P.N. Gelat, A novel sensor for monitoring acoustic cavitation. Part II: prototype performance evaluation, *IEEE Trans. Ultrason. Ferroelectr. Freq. Control* 50 (2003) 1351–1362, <https://doi.org/10.1109/TUFFC.2003.1244752>.
- [3] M. Hodnett, R. Chow, B. Zeqiri, High-frequency acoustic emissions generated by a 20 kHz sonochemical horn processor detected using a novel broadband acoustic

- sensor: a preliminary study, *Ultrason. Sonochem.* 11 (2004) 441–454, <https://doi.org/10.1016/j.ulsonch.2003.09.002>.
- [4] Y. Seto, N. Kawashima, M.K. Kurosawa, S. Takeuchi, Fundamental study of cavitation sensors fabricated with lead zirconate titanate film deposited by hydrothermal method: analysis and consideration of output signal from the sensor, *Jpn. J. Appl. Phys.* 47 (2008) 3871–3873, <https://doi.org/10.1143/JJAP.47.3871>.
- [5] T. Uchida, H. Sato, S. Takeuchi, T. Kikuchi, Investigation of output signal from cavitation sensor by dissolved oxygen level and sonochemical luminescence, *Jpn. J. Appl. Phys.* 49 (2010) 07HE03, <https://doi.org/10.1143/JJAP.49.07HE03>.
- [6] T. Uchida, S. Takeuchi, T. Kikuchi, Measurement of amount of generated acoustic cavitation: investigation of spatial distribution of acoustic cavitation generation using broadband integrated voltage, *Jpn. J. Appl. Phys.* 50 (2011) 07HE01, <https://doi.org/10.1143/JJAP.50.07HE01>.
- [7] T. Uchida, S. Takeuchi, T. Kikuchi, Measurement of spatial distribution in vertical direction of cavitation generation by using high resolution cavitation sensor, *Jpn. J. Appl. Phys.* 51 (2012) 07GD03, <https://doi.org/10.1143/JJAP.51.07GD03>.
- [8] T. Uchida, Quantitative evaluation of ultrasonic cleaning ability using acoustic cavitation signal, *Jpn. J. Appl. Phys.* 60 (2021) SDD04. 10.35848/1347-4065/abc5d.
- [9] I. Tzanakis, M. Hodnett, G.S.B. Lebon, N. Dezhkunov, D.G. Eskin, Calibration and performance assessment of an innovative high-temperature cavimeter, *Sens. Actuators A* 240 (2016) 57–69, <https://doi.org/10.1016/j.sna.2016.01.024>.
- [10] K. Johansen, J.H. Song, P. Prentice, Performance characterization of a passive cavitation detector optimized for subharmonic periodic shock waves from acoustic cavitation in MHz and sub-MHz ultrasound, *Ultrason. Sonochem.* 43 (2018) 146–155, <https://doi.org/10.1016/j.ulsonch.2018.01.007>.
- [11] V. Bull, J. Civalé, I. Rivens, G.ter Harr., A comparison of acoustic cavitation detection thresholds measured with piezo-electric and fiber-optic hydrophone sensors, *Ultrason. Sonochem.* 39 (2013) 2406–2421, <https://doi.org/10.1016/j.ultrasmedbio.2013.06.010>.
- [12] Z. Kyriakou, M.I. Corral-Baques, A. Amat, C.C. Coussios, HIFU-induced cavitation and heating in ex vivo porcine subcutaneous fat, *Ultrason. Sonochem.* 37 (2011) 568–579, <https://doi.org/10.1016/j.ultrasmedbio.2011.01.001>.
- [13] J.P. Koulakis, J. Rouch, N. Huynh, G. Dubrovsky, J.C.Y. Dunn, Interstitial matrix prevents therapeutic ultrasound from causing inertial cavitation in tumescent subcutaneous tissue, *Ultrason. Sonochem.* 44 (2018) 177–186, <https://doi.org/10.1016/j.ultrasmedbio.2017.09.005>.
- [14] G.S.B. Lebon, I. Tzanakis, K. Pericleous, D. Eskin, Experimental and numerical investigation of acoustic pressures in different liquids, *Ultrason. Sonochem.* 42 (2018) 411–421, <https://doi.org/10.1016/j.ulsonch.2017.12.002>.
- [15] C.D. Arvanitis, M. Bazan-Peregrino, B. Pifai, L.W. Seymour, C.C. Coussios, Cavitation-enhanced extravasation for drug delivery, *Ultrason. Sonochem.* 37 (2011) 1838–1852, <https://doi.org/10.1016/j.ultrasmedbio.2011.08.004>.
- [16] M. Hauptmann, S. Brems, H. Struyf, P. Mertens, M. Heyns, S. De Gendt, C. Glorieux, Time-resolved monitoring of cavitation activity in megasonic cleaning systems, *Rev. Sci. Instrum.* 83 (2012), 034904, <https://doi.org/10.1063/1.3697710>.
- [17] M. Hauptmann, H. Struyf, P. Mertens, M. Heyns, S. De Gendt, C. Glorieux, S. Brems, Towards an understanding and control of cavitation activity in 1 MHz ultrasound fields, *Ultrason. Sonochem.* 20 (2013) 77–88, <https://doi.org/10.1016/j.ulsonch.2012.05.004>.
- [18] T.T. Nguyen, Y. Asakura, S. Koda, K. Yasuda, Dependence of cavitation, chemical effect, and mechanical effect thresholds on ultrasonic frequency, *Ultrason. Sonochem.* 39 (2017) 301–306, <https://doi.org/10.1016/j.ulsonch.2017.04.037>.
- [19] T.T. Nguyen, Y. Asakura, N. Okada, S. Koda, K. Yasuda, Effect of ultrasonic cavitation on measurement of sound pressure using hydrophone, *Jpn. J. Appl. Phys.* 56 (2017) 07JE06, <https://doi.org/10.7567/JJAP.56.07JE06>.
- [20] D.M. Hallow, A.D. Mahajan, T.E. McCutchen, M.R. Prausnitz, Measurement and correlation of acoustic cavitation with cellular bioeffects, *Ultrason. Sonochem.* 32 (2006) 1111–1122, <https://doi.org/10.1016/j.ultrasmedbio.2006.03.008>.
- [21] G. Haar, C. Coussios, High intensity focused ultrasound: physical principles and devices, *Int. J. Hyperthermia* 23 (2007) 89–104, <https://doi.org/10.1080/02656730601186138>.
- [22] J.J. Kwan, S. Graham, R. Myers, R. Carlisle, E. Stride, C.C. Coussios, Ultrasound-induced inertial cavitation from gas-stabilizing nanoparticles, *Phys. Rev. E* 92 (2015), 023019, <https://doi.org/10.1103/PhysRevE.92.023019>.
- [23] E. Lyka, C. Coviello, R. Kozick, C.C. Coussios, Sum-of-harmonics method for improved narrowband and broadband signal quantification during passive monitoring of ultrasound therapies, *J. Acoust. Soc. Am.* 140 (2016) 741–754, <https://doi.org/10.1121/1.4958991>.
- [24] J. Frohly, S. Labouret, C. Bruneel, I. Looten-Baquet, T. Torguet, Ultrasonic cavitation monitoring by acoustic noise power measurement, *J. Acoust. Soc. Am.* 108 (2000) 2012–2020, <https://doi.org/10.1121/1.1312360>.
- [25] W. Lauterborn, E. Cramer, Subharmonic route to chaos observed in acoustics, *Phys. Rev. Lett.* 47 (1981) 1445–1448, <https://doi.org/10.1103/PhysRevLett.47.1445>.
- [26] T.D. Mast, V.A. Salgaonkar, C. Karunakaran, J.A. Besse, S. Datta, C.K. Holland, Acoustic emissions during 3.1 MHz ultrasound bulk ablation in vitro, *Ultrason. Sonochem.* 34 (2008) 1434–1448, <https://doi.org/10.1016/j.ultrasmedbio.2008.02.007>.
- [27] P.M. Seya, C. Desjouis, J.-C. Bera, C. Insera, Hysteresis of inertial cavitation activity induced by fluctuating bubble size distribution, *Ultrason. Sonochem.* 27 (2015) 262–267, <https://doi.org/10.1016/j.ulsonch.2015.05.036>.
- [28] E.A. Neppiras, Measurement of acoustic cavitation, *IEEE Trans. Sonics Ultrason.* SU-15 (1968) 81–88, <https://doi.org/10.1109/T-SU.1968.29452>.
- [29] T. Tuziuti, K. Yasui, M. Sivakumar, Y. Iida, N. Miyoshi, Correlation between acoustic cavitation noise and yield enhancement of sonochemical reaction by particle addition, *J. Phys. Chem. A* 109 (2005) 4869–4872, <https://doi.org/10.1021/jp0503516>.
- [30] G.J. Price, M. Ashokkumar, M. Hodnett, B. Zequiri, F. Grieser, Acoustic emission from cavitating solutions: implications for the mechanisms of sonochemical reactions, *J. Phys. Chem. B* 109 (2005) 17799–17801, <https://doi.org/10.1021/jp0543227>.
- [31] Z. Zhang, X. Liu, D. Li, Y. Lei, T. Gao, B. Wu, J. Zhao, Y. Wang, G. Zhou, H. Yao, Mechanism of ultrasonic impregnation on porosity of activated carbons in non-cavitation and cavitation regimes, *Ultrason. Sonochem.* 51 (2019) 206–213, <https://doi.org/10.1016/j.ultrasmedbio.2018.10.024>.
- [32] J.H. Song, A. Moldovan, P. Prentice, Non-linear acoustic emissions from therapeutically driven contrast agent microbubbles, *Ultrason. Sonochem.* 45 (2019) 2188–2204, <https://doi.org/10.1016/j.ultrasmedbio.2019.04.005>.
- [33] J.H. Song, K. Johansen, P. Prentice, An analysis of the acoustic cavitation noise spectrum: the role of periodic shock waves, *J. Acoust. Soc. Am.* 140 (2016) 2494–2505, <https://doi.org/10.1121/1.4964633>.
- [34] L. Yusuf, M.D. Symes, P. Prentice, Characterising the cavitation activity generated by an ultrasonic horn at varying tip-vibration amplitudes, *Ultrason. Sonochem.* 70 (2021), 105273, <https://doi.org/10.1016/j.ulsonch.2020.105273>.
- [35] N.V. Malykh, G.N. Sankin, Stabilization and acoustic spectra of a cavitation cluster in an ultrasonic spherical cavity, *Tech. Phys.* 55 (2010) 92–97, <https://doi.org/10.1134/S1063784210010159>.
- [36] C. Koch, Sound field measurement in a double layer cavitation cluster by rugged miniature needle hydrophones, *Ultrason. Sonochem.* 29 (2016) 439–446, <https://doi.org/10.1016/j.ulsonch.2014.05.018>.
- [37] D. Qin, Q. Zou, S. Lei, W. Wang, Z. Li, Nonlinear dynamics and acoustic emissions of interacting cavitation bubbles in viscoelastic tissues, *Ultrason. Sonochem.* 78 (2021), 105712, <https://doi.org/10.1016/j.ulsonch.2021.105712>.
- [38] S. Behnia, M. Yahyavi, R. Habibpourbisfar, Association schemes perspective of microbubble cluster in ultrasonic fields, *Ultrason. Sonochem.* 44 (2018) 45–52, <https://doi.org/10.1016/j.ulsonch.2018.02.006>.
- [39] E.A. Neppiras, Subharmonic and other low-frequency emission from bubbles in sound-irradiated liquids, *J. Acoust. Soc. Am.* 46 (1969) 587–601, <https://doi.org/10.1121/1.1911735>.
- [40] V.I. Ilyichev, V.L. Koretz, N.P. Melnikov, Spectral characteristics of acoustic cavitation, *Ultrasonics* 27 (1989) 357–361, [https://doi.org/10.1016/0041-624X\(89\)90034-6](https://doi.org/10.1016/0041-624X(89)90034-6).
- [41] Y. An, Nonlinear bubble dynamics of cavitation, *Phys. Rev. E* 85 (2012), 016305, <https://doi.org/10.1103/PhysRevE.85.016305>.
- [42] K. Yasui, T. Tuziuti, J. Lee, T. Kozuka, A. Towata, Y. Iida, Numerical simulations of acoustic cavitation noise with the temporal fluctuation in the number of bubbles, *Ultrason. Sonochem.* 17 (2010) 460–472, <https://doi.org/10.1016/j.ulsonch.2009.08.014>.
- [43] K. Yasui, *Acoustic Cavitation and Bubble Dynamics*, Springer, Cham, Switzerland, 2018, <https://doi.org/10.1007/978-3-319-68237-2>.
- [44] M.P. Brenner, S. Hilgenfeldt, D. Lohse, Single-bubble sonoluminescence, *Rev. Mod. Phys.* 74 (2002) 425–484, <https://doi.org/10.1103/RevModPhys.74.425>.
- [45] K. Yasui, Dynamics of acoustic bubbles, in: F. Grieser, P. Choi, N. Enomoto, H. Harada, K. Okitsu, K. Yasui (Eds.), *Sonochemistry and the Acoustic Bubble*, Elsevier, Amsterdam, 2015, pp. 41–83, <https://doi.org/10.1016/B978-0-12-801530-8.00003-7>.
- [46] Y.T. Didenko, W.B. McNamara III, K.S. Suslick, Temperature of multibubble sonoluminescence in water, *J. Phys. Chem. A* 103 (1999) 10783–10788, <https://doi.org/10.1021/jp991524s>.
- [47] W.B. McNamara III, Y.T. Didenko, K.S. Suslick, Pressure during sonoluminescence, *J. Phys. Chem. B* 107 (2003) 7303–7306, <https://doi.org/10.1021/jp034236b>.
- [48] K. Yasui, Multibubble sonoluminescence from a theoretical perspective, *Molecules* 26 (2021) 4624, <https://doi.org/10.3390/molecules26154624>.
- [49] K. Yasui, Production of O radicals from cavitation bubbles under ultrasound, *Molecules* 27 (2022) 4788, <https://doi.org/10.3390/molecules27154788>.
- [50] K. Yasui, Unsolved problems in acoustic cavitation, in: M. Asokkumar, F. Cavaliere, F. Chemat, K. Okitsu, A. Sambandam, K. Yasui, B. Zisu (Eds.), *Handbook of Ultrasonics and Sonochemistry*, Springer, Singapore, 2016, pp. 259–292, https://doi.org/10.1007/978-981-287-278-4_1.
- [51] K. Yasui, Y. Iida, T. Tuziuti, T. Kozuka, A. Towata, Strongly interacting bubbles under an ultrasonic horn, *Phys. Rev. E* 77 (2008), 016609, <https://doi.org/10.1103/PhysRevE.77.016609>.
- [52] K. Yasui, J. Lee, T. Tuziuti, A. Towata, T. Kozuka, Y. Iida, Influence of the bubble-bubble interaction on destruction of encapsulated microbubble under ultrasound, *J. Acoust. Soc. Am.* 126 (2009) 973–982, <https://doi.org/10.1121/1.3179677>.
- [53] K. Yasui, A. Towata, T. Tuziuti, T. Kozuka, K. Kato, Effect of static pressure on acoustic energy radiated by cavitation bubbles in viscous liquids under ultrasound, *J. Acoust. Soc. Am.* 130 (2011) 3233–3242, <https://doi.org/10.1121/1.3626130>.
- [54] Y. Fan, H. Li, J. Zhu, W. Du, A simple model of bubble cluster dynamics in an acoustic field, *Ultrason. Sonochem.* 64 (2020), 104790, <https://doi.org/10.1016/j.ulsonch.2019.104790>.
- [55] Y. Shen, L. Zhang, Y. Wu, W. Chen, The role of the bubble-bubble interaction on radial pulsations of bubbles, *Ultrason. Sonochem.* 73 (2021), 105535, <https://doi.org/10.1016/j.ulsonch.2021.105535>.
- [56] T.J. Matula, S.M. Cordry, R.A. Roy, L.A. Crum, Bjerknes force and bubble levitation under single-bubble sonoluminescence conditions, *J. Acoust. Soc. Am.* 102 (1997) 1522–1527, <https://doi.org/10.1121/1.420065>.
- [57] T.J. Matula, I.M. Hallaj, R.O. Cleveland, L.A. Crum, W.C. Moss, R.A. Roy, The acoustic emissions from single-bubble sonoluminescence, *J. Acoust. Soc. Am.* 103 (1998) 1377–1382, <https://doi.org/10.1121/1.421279>.
- [58] F.R. Young, *Sonoluminescence*, CRC Press, Boca Raton, 2005.

- [59] K. Yasui, T. Tuziuti, M. Sivakumar, Y. Iida, Sonoluminescence, *Appl. Spectrosc. Rev.* 39 (2004) 399–436, <https://doi.org/10.1081/ASR-200030202>.
- [60] W. Lauterborn, T. Kurz, R. Mettin, C.D. Ohl, Experimental and theoretical bubble dynamics, in: I. Prigogine, S.A. Rice (Eds.), *Advances in Chemical Physics*, vol. 110, John Wiley & Sons, 1999, pp. 295–380, <https://doi.org/10.1002/9780470141694.ch5>.
- [61] J. Holzfuss, M. Ruggeberg, A. Billo, Shock wave emissions of a sonoluminescing bubble, *Phys. Rev. Lett.* 81 (1998) 5434–5437, <https://doi.org/10.1103/PhysRevLett.81.5434>.
- [62] K. Negishi, Experimental studies on sonoluminescence and ultrasonic cavitation, *J. Phys. Soc. Jpn.* 16 (1961) 1450–1465, <https://doi.org/10.1143/JPSJ.16.1450>.
- [63] R. Hickling, M.S. Plesset, Collapse and rebound of a spherical bubble in water, *Phys. Fluids* 7 (1964) 7–14, <https://doi.org/10.1063/1.1711058>.
- [64] K. Naugolnykh, L. Ostrovsky, *Nonlinear Wave Processes in Acoustics*, Cambridge Univ. Press, Cambridge, UK, 1998.
- [65] M.F. Hamilton, D.T. Blackstock (Eds.), *Nonlinear Acoustics*, Academic Press, San Diego, USA, 1998.
- [66] P.K. Kundu, *Fluid Mechanics*, Academic Press, San Diego, USA, 1990.
- [67] W. Lauterborn, E. Suchla, Bifurcation superstructure in a model of acoustic turbulence, *Phys. Rev. Lett.* 53 (1984) 2304–2307, <https://doi.org/10.1103/PhysRevLett.53.2304>.
- [68] W. Lauterborn, T. Kurz, I. Akhatov, Nonlinear acoustics in fluids, in: T.D. Rossing (Ed.), *Springer Handbook of Acoustics*, Springer, New York, 2007, pp. 257–297.
- [69] W. Lauterborn, T. Kurz, Physics of bubble oscillations, *Rep. Prog. Phys.* 73 (2010), 106501, <https://doi.org/10.1088/0034-4885/73/10/106501>.
- [70] S.H. Strogatz, *Nonlinear Dynamics and Chaos: with Applications to Physics, Biology, Chemistry, and Engineering*, 2nd ed., CRC Press, Boca Raton, USA, 2018.
- [71] K. Yasui, Influence of ultrasonic frequency on multibubble sonoluminescence, *J. Acoust. Soc. Am.* 112 (2002) 1405–1413, <https://doi.org/10.1121/1.1502898>.
- [72] J. Lee, M. Ashokkumar, S. Kentish, F. Grieser, Determination of the size distribution of sonoluminescence bubbles in a pulsed acoustic field, *J. Am. Chem. Soc.* 127 (2005) 16810–16811, <https://doi.org/10.1021/ja0566432>.
- [73] D. Sunartio, M. Ashokkumar, F. Grieser, Study of the coalescence of acoustic bubbles as a function of frequency, power, and water-soluble additives, *J. Am. Chem. Soc.* 129 (2007) 6031–6036, <https://doi.org/10.1021/ja068980w>.
- [74] S. Luther, M. Sushchik, U. Parlitz, I. Akhatov, W. Lauterborn, Is cavitation noise governed by a low-dimensional chaotic attractor?, in: W. Lauterborn, T. Kurz (Eds.), *Nonlinear Acoustics at the Turn of the Millennium: ISNA 15, AIP Conf. Proc. No. 524* American Institute of Physics, New York, 2000, pp. 355–358.
- [75] A. Prosperetti, *Advanced Mathematics for Applications*, Cambridge Univ. Press, Cambridge, 2011.
- [76] W. Lauterborn, R. Mettin, Acoustic cavitation: bubble dynamics in high-power ultrasonic fields, in: J.A. Gallego-Juarez, K.F. Graff (Eds.), *Power Ultrasonics*, Elsevier, Amsterdam, 2015, pp. 37–78, <https://doi.org/10.1016/B978-1-78242-028-6.00003-X>.
- [77] M. Arora, C.D. Ohl, D. Lohse, Effect of nuclei concentration on cavitation cluster dynamics, *J. Acoust. Soc. Am.* 121 (2007) 3432–3436, <https://doi.org/10.1121/1.2722045>.
- [78] I. Hansson, K.A. Morch, The dynamics of cavity clusters in ultrasonic (vibratory) cavitation erosion, *J. Appl. Phys.* 51 (1980) 4651–4658, <https://doi.org/10.1063/1.328335>. Conflict of interest.